SLOPE FAILURE EVALUATION BY ENERGY APPROACH IN HYDRAULIC FILL DAMS DUE TO LIQUEFACTION-INDUCED WATER FILMS

Takaji KOKUSHO[1] and Kazuhiro KABASAWA[2]

SUMMARY

Earth dams constructed by hydraulically filling methods are composed of loose sandy soils with laminations of different particle sizes. If such fill materials liquefy during strong earthquakes, the void redistribution effect becomes dominant to generate water films beneath less permeable layers, which will destabilize dam slopes in a greater extent than uniform soil materials. An energy approach is proposed in which flow deformation of dam slopes is evaluated considering the water film effect. The residual shear strength exerted along the water film is evaluated about 20% of uniform sand according to the energy approach applied to model shaking table tests.

Key Words: hydraulic fill dam, earthquake, liquefaction, void redistribution, energy approach, residual strength

INTRODUCTION

Earth dams constructed in old days by hydraulically filling methods are composed of loose sandy soils with laminations of different particle sizes. If such fill materials liquefy during strong earthquakes, the void redistribution effect is likely to dominate and generate water films beneath less permeable layers, which will destabilize dam slopes in a greater extent than uniform soil materials. The failure of the Lower San Fernando dam during the 1973 San Fernando earthquake (Seed [1]) may have been the case. In the first part of this paper, previous research results on void redistribution or water films obtained by the present authors by means of in situ soil investigations, model tests, etc. are

_____

1. Professor, Chuo University, Tokyo, Japan, Email: kokusho@civil.chuo-u.ac.jp

2. Ph.D. student, ditto

summarized to demonstrate how laminated sandy slopes are vulnerable to flow failures involving water films.

At this moment, no reasonable method is available for evaluating flow displacement of earth dam slopes considering weak zones such as water films. Therefore, an energy approach is proposed for evaluation of post-shaking slope displacement considering the effect of reduced shear strength due to void redistribution effect. Based on the energy approach, residual strength mobilized on a slip surface along water film is back-calculated from model test results for rough estimation of reduction in shear strength due to void redistribution effect.

PREVIOUS RESEARCH RESULTS ON VOID REDISTRIBUTION OR WATER FILMS

The significant effect of void redistribution or water films in layered sand deposits has already been demonstrated by a series of model tests and case studies by Kokusho and his research group [2-7]. The followings are major findings in the research.

Site investigation was carried out at a deep dewatered excavation in hydraulically filled ground along the Tokyo Bay shown in the photograph of Fig.1. Soils were sampled slice by slice by 2 cm thickness at the excavation slope. Fig.2 shows the percentage of soil content for four different soil particles. It was found that sandy soil was very variable in terms of particle size along the depth as indicated in Fig.2. The contents corresponding to the mesh size of 0.075 mm and 0.106 mm are fluctuating almost periodically by intervals shorter than 2 m. The continuation of this periodical fluctuation could be

Fig.1 Excavation slope in reclaimed ground showing lamination of sublayers
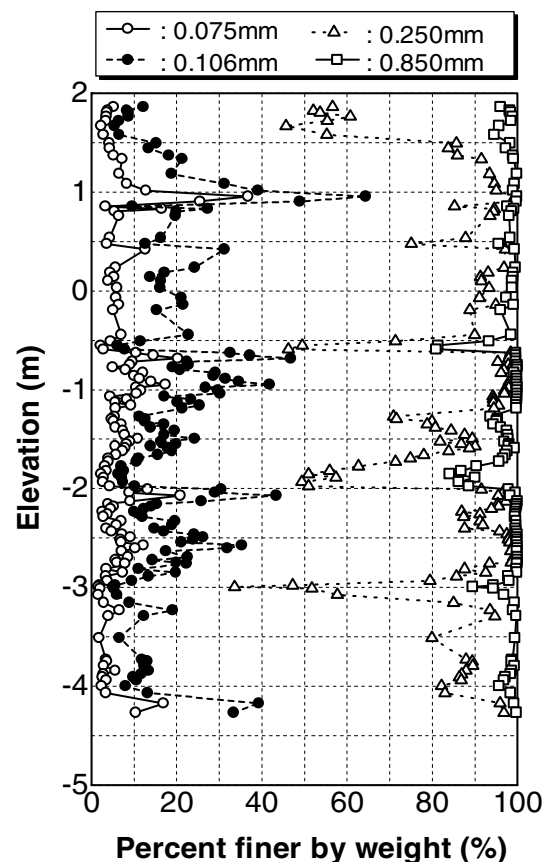

Fig.2 Sieving test results in reclaimed ground along the Tokyo Bay constructed by hydraulic filling

easily identified in the site as indicated in the photograph. Several silt seams could be traced in a distance longer than 20 or 30 m in the horizontal direction. Another site investigation was performed in alluvial sand deposits in Niigata, which showed less frequent inclusion of fine soil seams though some thicker silt seams were still there. Thus, it may well be assumed that the hydraulic filling method tends to generate more laminations of variable soil particles than natural ground.

Post-liquefaction behavior in saturated layered sand was measured in a lucite tube of 13.0cm in inner diameter and 211.5cm in height [2, 3, 4]. The one-dimensional sand layer was instantaneously liquefied by an impact given to the tube base by a steel hammer powered by a controlled spring force. Four different types of layered models shown in Fig.3 were constructed in the tube. In Model 1, the sand layer of 200cm in depth sandwiching a seam of non-plastic silt in the middle, Model 2 consisting of upper fine sand and lower coarse sand, Model 3 consisting of upper and lower coarse sands and middle sandwiched fine sand and Model 4 almost identical with Model 2 except that water

Fig.3 Four types of 1-dimensional layered soil models in the tube

Fig.4 Stable water film generation mechanism

table standing in the middle of the upper fine sand layer. Thicknesses and relative densities of individual layers are available in Fig.3. In summary, stable water film was formed in most cases except in Model 2 at or near the lower boundary of the low permeability layer because high hydraulic gradient was introduced in the low permeability layer. Thus the mechanism for generating stable water film is so simple as indicated in Fig.4 in which the hydraulic gradient introduced in the middle layer, i_m, is expressed by the equation;
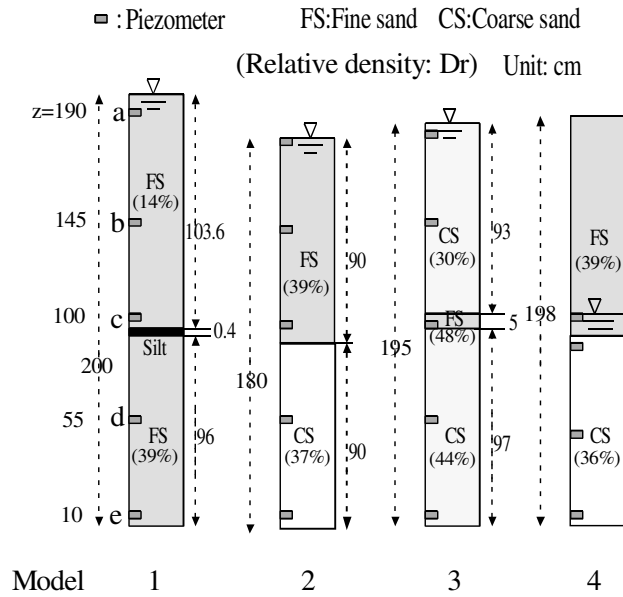
$$i_m = \frac{(\gamma'_u H_u + \gamma'_m H_m) - (\gamma'_u H_u - s')}{\gamma_w H_m} = i_{cr} + \frac{s'}{\gamma_w H_m} \qquad (1)$$

where $i_{cr} = \gamma'_m / \gamma_w$ is the critical hydraulic gradient, $s' =$ the effective stress recovered at the bottom of the upper layer, i_m, $i_u =$ the hydraulic gradients in the middle and upper layer, respectively, H_m, $H_u =$ the thickness of those layers, γ'_m, $\gamma'_u =$ the buoyant unit weights of those layers and $\gamma_w =$ the unit weight of water. The series of test results clearly indicated that a water film is readily formed just after the onset of liquefaction beneath a sandwiched sublayer with smaller permeability and stays there much longer than re-sedimentation of liquefied sand particles. This indicates that the liquefied sand is actually in the drained condition locally, allowing the void redistribution to occur. Soil layering structures providing this mechanism seem to be abundant in the field introducing multiple water films at different depths. Even if stable water films did not appear in the test results of Model 2, transient turbulence took place leading to zones of larger void ratio near the boundary of sand sublayers which may temporarily serve as a slip surface. Thus, the void redistribution effect, stable water films or transient turbulence, will no doubt provide weak zones for sliding if the soil has a potential for lateral flow.
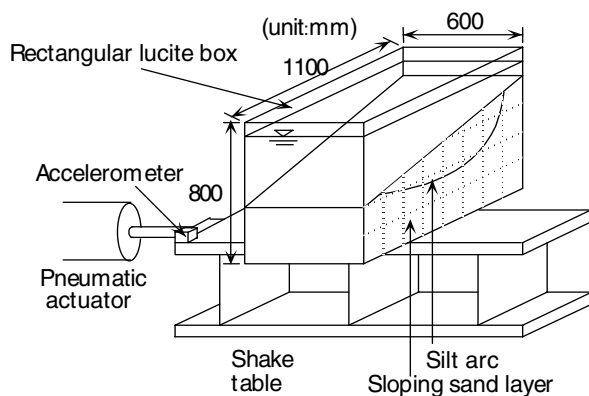

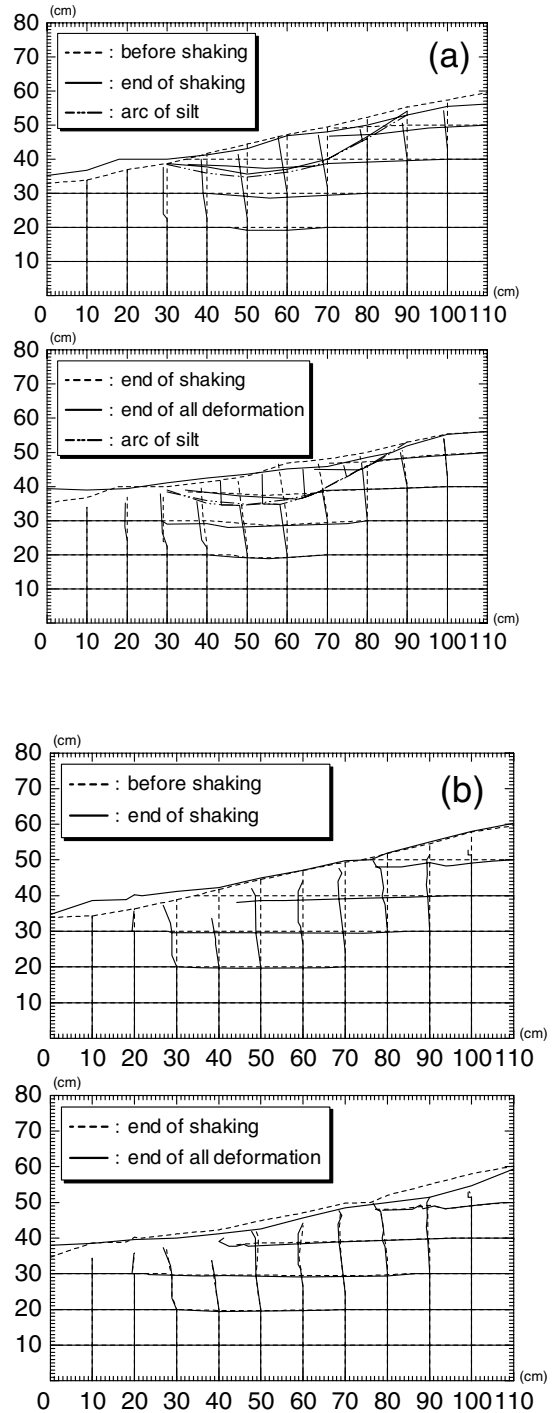Fig.5 Shake table test for saturated sand slope with silt arc

Fig.6 Cross-sectional deformation for slopes with silt arc (a) and without silt arc (b)
Top of (a) and (b): during shaking
Bottom of (a) and (b): after shaking

In order to know the effect of initial shear stress given by a slope on the void redistribution and slope instability, 2-dimensional shaking table tests were performed as shown in Fig.5. Clean fine sand was rained in water to make a saturated loose sand slope of relative density of 20-36% in a rectangular soil box in which an arc-shaped silt seam was placed. The model was subjected to 3 cycles of sinusoidal shaking perpendicular or parallel to the sloping direction and the flow movement was observed through the transparent side wall. Video movies of the tests are accessible at the web site;

http//:www.civil.chuo-u.ac.jp/lab/doshitu/index.html

Fig.6(a) indicates that the flow deformation occurs not only during shaking but also after the end of shaking along the silt arc beneath which thin water film could be recognized. The post-shaking flow occurs almost exclusively along the slip surface quite discontinuously. In contrast, Fig.6(b) indicates that flow deformation in a uniform sand model occurs mostly during shaking. Time histories of the same test results are shown in Fig. 7. In Fig.7(a) without the silt seam, flow occurs only during shaking, but in Fig.7(b) with the silt arc, large flow also occurs after shaking. The target points on the charts are shown in Fig. 7(d). These results are for the table acceleration of 0.31 G. In Fig.7(c), the time histories of flow deformation of the same model subjected to

Fig.7 Time-dependent flow displacement at target points shown in (d); without silt arc by Acc. 0.34 G (a), with silt arc by Acc 0.34 G (b) and with silt arc by Acc. 0.18 G (c).

weaker acceleration of 0.18G are shown. In this case, much larger post-shaking flow occurs than the case of 0.34G while minimal deformation takes place during shaking. This is because in the weaker acceleration, the slope remains steep during shaking and so larger driving forces are sustained in post-shaking flow along the water film as demonstrated by Kabasawa and Kokusho [8].
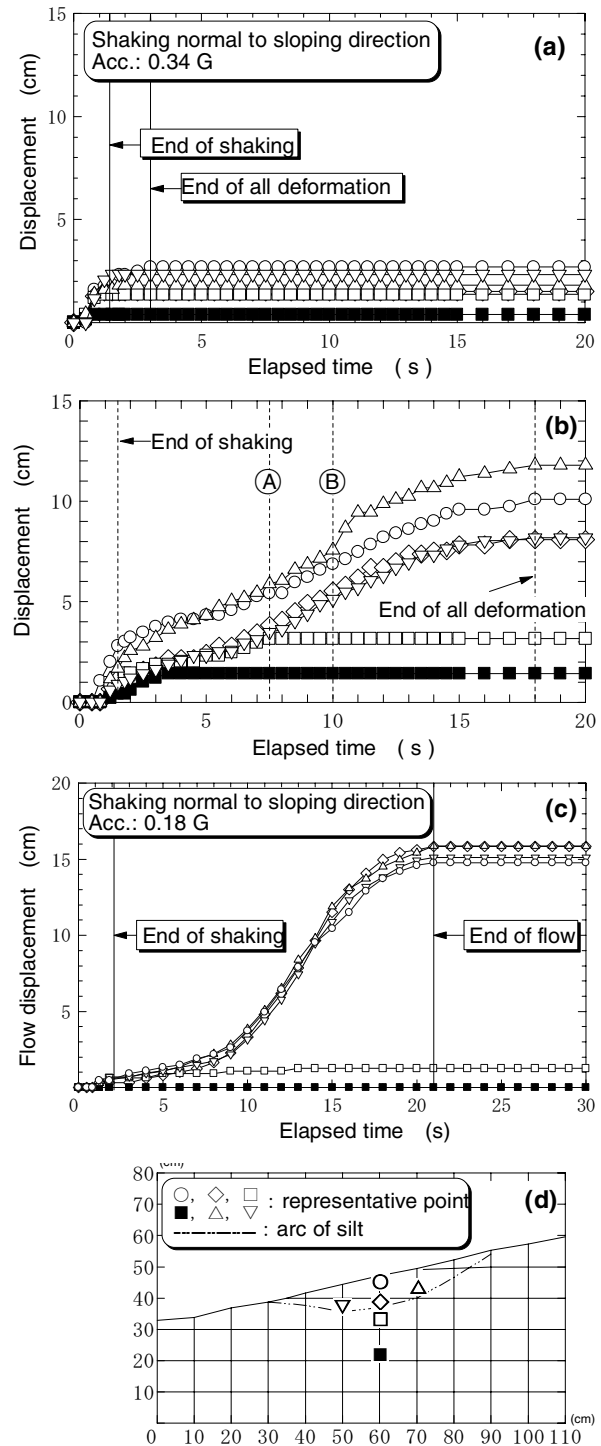
2D shake table tests were carried out also for other slope models of different configurations, in all of which analogous delayed sliding was recognized in cases with sandwiched silt seams in saturated sand slopes. Based on the comparative observation of the cases with and without a silt seam, it was pointed out that a water film formed beneath the seam serves as a shear stress isolator which shields the deeper soil from the development of shear strain and dilatancy [4]. Consequently, the sand mass can experience large slide beneath the silt seam without suffering from the dilatancy of underlying sand, whereas a uniform sand slope stops moving after the end of shaking. Considering that no such large post-shaking failure occurs in the uniform sand slope, a significant effect of the void redistribution or water film formation is demonstrated at least qualitatively.

Fig.8 Energy balance in seismically induced slope failure
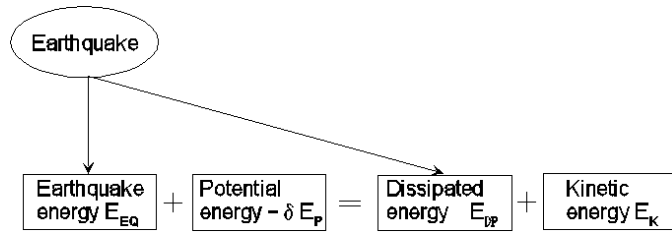
ENERGY APPROACH FOR SLOPE FAILURE EVALUATION

Slope failures have been evaluated based on the equilibrium of forces acting on a potentially sliding soil mass. This force approach can evaluate the initiation of slide or the safety factor against the slope failure, though it cannot predict large flow deformation once the failure starts. From the viewpoint of the performance based design or the risk evaluation of old dams under severe seismic motions for retrofitting, it is immensely important to evaluate not only the safety factor but also how large deformation will develop and how far its effect reaches downslope. In this research, an energy approach first proposed by Kokusho and Kabasawa [9] is introduced to evaluate failure deformation considering the effect of reduced shear strength due to void redistribution effect.

The basic idea is shown in Fig.8. In case of earthquake-induced slope failures, four energies; potential energy by the gravity E_p, kinetic energy E_k of sliding soil mass, earthquake energy contributing to the slope failure E_{EQ} and energy dissipated in soil due to the slope deformation E_{DP}, can be correlated by the following equation [10];

$$E_{DP} + E_k = E_{EQ} - \delta E_p \qquad (2)$$

or in an incremental form as;

$$E_{DP} + E_k = E_{EQ} - \delta E_p \qquad (2a)$$

Note that the potential energy change before and after failure δE_p in Eq(2) or δE_p in Eq.(2a) is normally negative. If failures occur after the end of earthquake shaking as often observed in case

histories and also in the aforementioned shake table tests involving water films, the energy balance becomes identical with that in slope failures due to non-seismic causes without the earthquake energy;

$$E_{DP} + E_k = - \delta E_p \qquad (3)$$

If $- \delta E_p$ is larger than E_{DP} in Eq.(3), then $E_k > 0$ and failure starts. Namely the condition for initiation of failure is;

$$E_k = - \delta E_p - E_{DP} > 0 \qquad \text{or} \quad - \delta E_p > E_{DP} \qquad (4)$$

Once failure starts, the amount of the dissipated energy is critical to decide if it gains speed and how far it flows. If E_{DP} is smaller than $- \delta E_p$ in some time increments, then E_k is increased and the soil movement is accelerated. The acceleration may occur not only due to increase in $- \delta E_p$ but also due to drastic decrease of E_{DP} caused by pore-pressure buildup or appearance of weak zones such as water films in liquefiable sand deposits. A soil mass can keep moving unless the kinetic energy at a time (E_k) plus the subsequent potential energy change ($-\delta E_p$) is all dissipated. If $- \delta E_p$ is smaller than E_{DP}, then E_k is negative, hence the soil mass loses the speed and comes to a halt if reserved kinetic energy E_k is all consumed. If the failure mode and the energy dissipation mechanism in the moving soil mass are known, it will be possible to evaluate how far it will reaches in the down-slope direction [9].

Flow failures during earthquake shaking are more complex and have been discussed in another literature in comparison with the Newmark method [10]. However, as far as post-shaking flow failures are concerned, the energy balance in Eq.(3) can hold. Let us consider a two dimensional problem with coordinate axes x and z and let $u(x,z,t)$ and $w(x,z,t)$ be deformations along the two axes at time t. The incremental potential energy $- \delta E_p$ can be expressed as

$$- \delta E_p = \int (\rho_{sat} - \rho_w) \cdot g \cdot \{w(x,z,t + t) - w(x,z,t)\} dxdz \qquad (5)$$

where $w(x,z,t)$ is the vertical displacement of soil mass at a coordinate (x,z), t is a time increment, ρ_{sat} and ρ_w are densities of saturated soil and water, respectively, and g is the acceleration of gravity. Eq.(5) is applied to submerged saturated slopes. If sub-aerial unsaturated slopes are concerned, $(\rho_{sat} - \rho_w)$ in Eq.(5) is replaced by unsaturated density, ρ_t. The incremental kinetic energy is formulated as;

$$E_k = \int (\rho_{sat}/2) \{v^2(x,z,t + t) - v^2(x,z,t)\} dxdz \qquad (6)$$

where $v(x,z,t)$ is the particle velocity of soil at a coordinate (x,z) and calculated as

$$v(x,z,t) = \left\{ (\partial u / \partial t)^2 + (\partial w / \partial t)^2 \right\}^{1/2}. \tag{7}$$

If soil is unsaturated ρ_{sat} should be replaced by ρ_t. The increment of dissipated energy E_{DP} can be expressed as;

$$E_{DP} = \int \left\{ \tau(x,z,t) \; \gamma(x,z,t) + \sigma'(x,z,t) \; v(x,z,t) \right\} dx dz \tag{8}$$

where $\tau(x,z,t)$ and $\sigma'(x,z,t)$ are shear stress and isotropic effective stress components; $\tau = (\sigma'_x - \sigma'_z)/2$ and $\sigma' = (\sigma'_x + \sigma'_z)/2$ at a coordinate (x,z), respectively, and may be evaluated by stress analyses. Shear and volumetric strain increments, $\gamma(x,z,t)$ and $v(x,z,t)$, can be calculated from $u(x,z,t)$ and $w(x,z,t)$. The integrations in Eqs.(5), (6) and (8) should be implemented for a cross-sectional area where soil is influenced by the flow failure.

In actuality, Eqs.(5), (6) and (8) cannot be evaluated without knowing the failure mode of slopes. In a failure mode accompanying a distinct slip surface of an arc as a rigid body such as in the previously mentioned model tests, the equations are very much simplified. The potential and kinetic energies of Eqs.(5) and (6) can then be calculated as a rigid body movement and the dissipated energy of Eq.(8) can be calculated exclusively along the slip surface. The evaluation starts if Eq.(4) is satisfied and can be implemented step by step with a time increment t by resorting to Eqs.(5) to (8).

If the failure mode is spatially continuous, several continuous functions defining deformations $u_0(x,z)$, $w_0(x,z)$ on the x-z plane may be assumed considering the strain compatibility, boundary conditions, configurations and soil conditions of slopes, etc. Then, a small increment of vertical displacement $\delta w_0(x,z)$ is given, and the variation in the potential energy $- \delta E_p$ will be calculated accordingly by Eq.(5). Correspondingly the increment in the dissipated energy E_{DP} can be calculated by Eq.(8). Among the functions assumed, one which gives the smallest E_{DP} for the same $- \delta E_p$ will be chosen as an appropriate function simulating a probable failure mode. In some cases, a superposition of discontinuous and continuous modes may be considered feasible by adding the dissipated energies along the slip plane and in the deformed soil mass. The evaluation of the dissipated energy is very much influenced by stresses $\tau(x,z,t)$ or $\sigma'(x,z,t)$ in Eq.(8). In what follows, the energy approach is applied to the shake table test results mentioned previously to back-calculate residual strength exerted along the slip surface.

BACK-CALCULATION OF RESIDUAL STRENGTH IN MODEL TESTS

Let us apply the energy approach to the test result on two-dimensional flow failure shown in Fig.7(b). After the end of shaking, the soil mass above the silt arc starts to flow again without any inertia effect,

hence Eq.(3) holds (Kabasawa et al., 2002).　Between Point A and B in the figure, the flow velocity stays almost constant;

$$-\int_A^B \delta E_p = \int_A^B E_{DP} \quad \text{or} \quad E_{DP} = -\left(\delta E_{pA} - \delta E_{pB}\right) \tag{9}$$

indicating that the difference in potential energy between A and B is equal to the energy dissipated in the soil in the same time interval.　Because the corresponding soil flow can be approximated as a rigid body movement as substantiated in Fig.6(a), the energy is assumed to dissipate exclusively at the slip surface beneath the silt arc.　In order to calculate Eq.(9) the moving soil block may be sliced into vertical segments of n-pieces.　$-\delta E_p$ and E_{DP} can be calculated for a unit thickness of a slope as

$$-\delta E_p = \sum_{i=1}^n W_i\, w_i\,, \qquad E_{DP} = s \sum_{i=1}^n R_i l_i \tag{10}$$

respectively, where W_i = weight of the i'th segment (buoyant weight if submerged), w_i =incremental vertical displacement of the segment in a time increment, s =flow displacement tangent to the slip surface (assumed constant because of rigid body movement), R_i = resistant stress along the slip plane and l_i = segment length along the slip surface.　In sand without cohesion,

$$R_i = \sigma_i' \tan\phi' \tag{11}$$

may be assumed, where σ_i' =effective stress normal to the slip surface in the i'th segment and ϕ' =equivalent friction angle in terms of effective stress.

The equivalent friction angles ϕ' were evaluated by Eqs.(10) and (11) between two points, A and B as exemplified in Fig.7(b), where the displacement velocity was almost constant, from a series of tests　with various test conditions; the relative density of sand were 20% to 36%, the silt seam was either non-plastic or Ip=23, the table acceleration was 300 to 145 cm/s^2, two different model scales of 110 cm or 80 cm in the slope base length and the shaking direction is either perpendicular to or parallel with the sloping direction [8].　In　the　evaluation,　the
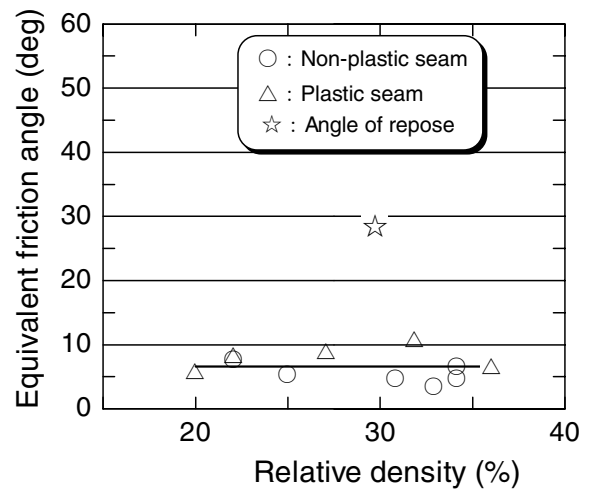

Fig.9 Equivalent friction angle versus relative density relationship

dissipated energy at both sides of the acrylic soil container was also taken into consideration by using $\mu K_0 =$0.125, which had been experimentally obtained by a tube test carried out by Kokusho and Kojima [6], where $\mu =$friction coefficient and $K_0 =$ earth-pressure coefficient between sand and acryl. The equivalent friction angle is evaluated as 5.3 to 10.7 degrees with the average 6.6 degrees. The star symbol in the figure indicates the angle of repose, $\phi' =$29 degrees, measured by statically inclining the submerged model slope [11]. Hence, the friction coefficient $\mu = \tan\phi'$ along the slip surface beneath the silt seam considerably decreases to about 20% on average of that for a homogeneous sand.

The plots in Fig.9 show no clear dependency on relative density, the plasticity of silt seams, the model dimension, etc., indicating that the residual strength along the slip surface is governed by factors insensitive to soil density or other test conditions probably because the water film basically dominates shear strength along the slip surface. However, it is evidently larger than zero. This non-zero strength cannot be explained if the slip surface actually passes all through continuous water film. The viscosity of thin water film seems to explain only one hundredth of the strength [9]. This is probably because the water film may be discontinuous or winding. More research is certainly needed to clarify the mechanism of residual strength mobilization along the slip surface just beneath silt seams. In the meantime, it may be possible to refer the results; residual strength is about 20% of initial value, in evaluating slope displacement along water films although the model is much smaller than prototype, because it is likely to capture the basic mechanism of sliding along water film in which effective stress is totally lost not only in the model but also in prototype.

CONCLUDING REMARKS

Several research findings for studying slope failures in hydraulically filled earth dams involving water films are addressed and an energy approach is proposed for evaluating flow displacements, yielding the following major conclusions.

1) Hydraulically filled ground consists of sublayers of sands and silts with different permeability which are continuous in the horizontal direction.

2) Sand deposits composed of sublayers of different permeability are prone to post-liquefaction void redistribution; stable water films or transient turbulence, which is likely to serve as a sliding surface or at least a part of it in flow failure even after the end of earthquake shaking.

3) In sand deposits including fine soil sublayers or seams, void redistribution or water film mechanism can facilitate large flow displacements without mobilizing dilatancy of underlying sand, while uniform sand deposit can only develop limited displacement because of the dilatancy effect even when relative density is rather low.

4) A basic idea on the energy approach has been proposed, in which flow displacement can be evaluated considering the balance between potential energy and dissipated energy in the displaced soil mass.

5) By applying the energy approach to shake table model test results, residual strength mobilized along the slip surface during post-shaking slope failure is back-calculated as about 20% of that of homogeneous sand irrespective of sand density, input accelerations, plasticity of silt seam and other test conditions.

REFERENCES

1. Seed, H. B. "Landslides during earthquakes due to soil liquefaction." *Proc. of American Society for Civil Engineers*, Vol.94, SM5, 1968: 1055-1122.

2. Kokusho, T., Watanabe, K. and Sawano, T. "Effect of water film on lateral flow failure of liquefied sand." *Proc. 11th European Conference on Earthquake Engineering*, Paris, CD publication, ECEE/T2/kokeow.pdf., 1998.

3. Kokusho,T. "Formation of water film in liquefied sand and its effect on lateral spread." *Journal of Geotechnical and Geoenvironmental Engineering*, American Society for Civil Engineers, Vol.125, No.10, 1999: 817-826.

4. Kokusho,T. "Mechanism for water film generation and lateral flow in liquefied sand layer." *Soils and Foundations*, Vol.40, No.5, 2000: 99-111.

5. Kokusho, T. "Failure mechanisms in liquefaction studied in recent earthquakes." *Proc. Satellite Conference on Earthquake Geotechnical Engineering*, International Conference on SMGE, Istanbul, 2001: 287-297.

6. Kokusho, T. and Kojima, T. "Mechanism for postliquefaction water film generation in layered sand" *Journal of Geotechnical and Geoenvironmental Engineering*, American Society for Civil Engineers, Vol.128, No.2, 2002: 129-137.

7. Kokusho, T. "Current state of research on flow failure considering void redistribution in liquefied deposits." *Soil Dynamics and Earthquake Engineering*, Elsevier, Vol.23, 2003: 585-603.

8. Kabasawa, K. and Kokusho, T. "Energy analysis and model tests on lateral flow induced by water film effect in liquefied ground." *Journal of Japan Society of Civil Engineers*, III, in print, 2004, (in Japanese).

9. T. Kokusho and K. Kabasawa, "Energy approach to flow failure and its application to flow due to water film in liquefied deposits," *Proc. of International Conference on Fast Slope Movement*, Naples, 2003: 297-302.

10. Kokusho, T., Ishizawa, T. and Harada, T. "Energy approach for earthquake induced slope failure evaluation." *Proc. 11th International Conference on Soil Dynamics & Earthquake Engineering and 3rd International Conference on Earthquake Geotechnical Engineering*, Berkeley, California, Vol.2, 2004: 260-267.

11. Kabasawa, K. and Kokusho. T. "Possibility of water film generation in saturated sand slope subjected to static loading." *Proc. Annual Convention of Japan Society of Civil Engineers*, Vol.3, 2001: 346-347, (in Japanese).